



Published in final edited form as:

Psychiatry Res. 2011 November 30; 194(2): 198–204. doi:10.1016/j.psychres.2011.05.003.

A mathematical formula for prediction of gray and white matter volume recovery in abstinent alcohol dependent individuals

Anderson Mon,

Department of Radiology and Biomedical Imaging, University of California, San Francisco and Center for Imaging of Neurodegenerative Diseases, Veterans Administration Medical Center San Francisco

Kevin Delucchi,

Department of Psychiatry, University of California, San Francisco

Timothy C. Durazzo,

Department of Radiology and Biomedical Imaging, University of California, San Francisco and Center for Imaging of Neurodegenerative Diseases, Veterans Administration Medical Center San Francisco

Stefan Gazdzinski, and

Center for Imaging of Neurodegenerative Diseases, Veterans Administration Medical Center San Francisco and M. Smoluchowski Institute of Physics, Jagiellonian University, Krakow, Poland

Dieter J. Meyerhoff

Department of Radiology and Biomedical Imaging, University of California, San Francisco and Center for Imaging of Neurodegenerative Diseases, Veterans Administration Medical Center San Francisco

Abstract

We propose a mathematical formula that predicts the trajectory of the recovery from lobar gray and white matter volume deficits in individuals with sustained abstinence from alcohol. The formula was validated by using MRI-measured volumetric data from 16 alcohol dependent individuals who had brain scans at three time points during abstinence from alcohol. Using the measured volumetric data of each individual from the first two time points, we estimated the individual's gray and white matter volume of the frontal, parietal and temporal lobes for the third time point using the formula. Similarly, using the measured data for the second and third time points, we estimated the first time point data for each individual. The data predicted from the formula were very similar to the experimentally measured data for all lobes and for both gray and white matter. The intra-class correlation coefficients between the measured data and the data estimated from the formula were > 0.95 for each tissue type. The formula may also be applicable in other neuroimaging studies of tissue volume changes such as white matter myelination during brain development and white matter demyelination or brain volume loss in neurodegenerative diseases, such as Alzheimer's disease.

Address for correspondence. Dr. Anderson Mon, Center for Imaging of Neurodegenerative Diseases, Veterans Administration Medical Center, Building 13, Mail Stop 114 M, 4150 Clement Street, San Francisco, CA 94121, Phone: 001-415-221-4810 x 2453, Fax: 001-415-668-2864, Anderson.Mon@ucsf.edu.

Publisher's Disclaimer: This is a PDF file of an unedited manuscript that has been accepted for publication. As a service to our customers we are providing this early version of the manuscript. The manuscript will undergo copyediting, typesetting, and review of the resulting proof before it is published in its final citable form. Please note that during the production process errors may be discovered which could affect the content, and all legal disclaimers that apply to the journal pertain.

Keywords

brain; MRI; atrophy; brain recovery; neurodegenerative disease; alcoholism

1. Introduction

Alcohol use disorders (AUD) and other substance use disorders (SUD) are associated with alterations of brain structure and function. Neuroimaging studies have consistently demonstrated gray matter (GM) and/or white matter (WM) loss and enlarged ventricles and sulci in AUD (Adalsteinsson and Spielman, 1999; Gazdzinski et al., 2005b; Jernigan et al., 1991; Pfefferbaum et al., 1996; Schroth et al., 1988; Sullivan et al., 1995; Zipursky et al., 1989) as well as with chronic cigarette smoking, amphetamine, cocaine and poly-substance use disorders (Brody et al., 2004; Durazzo and Meyerhoff, 2007; Liu et al., 1998; O'Neill et al., 2001).

Brain morphometric abnormalities in AUD demonstrate variable levels of recovery with sustained abstinence from alcohol (e.g., (Gazdzinski et al., 2005a)). Cross-sectional magnetic resonance imaging (MRI) studies of abstinent alcoholics demonstrated that those with smaller brain volumes at the inception of abstinence from alcohol recover faster than those with larger volumes at inception; and longitudinally, individual brain volume increases appear to be greater during short-term abstinence (i.e., the first few weeks) than during sustained long-term abstinence (Gazdzinski et al., 2005a; Pfefferbaum et al., 1995). These two observations suggest a non-linear trajectory of tissue volume recovery. The magnitude of volume change demonstrated with various morphometric MRI methods during both short-term and long-term abstinence from alcohol has been linked to the degree of tissue volume abnormalities at the beginning of abstinence (Cardenas et al., 2007; Gazdzinski et al., 2005a; Pfefferbaum et al., 1995; Yeh et al., 2007). Specifically, it was observed that individuals with greater GM and/or WM atrophy at the inception of abstinence (i.e., at baseline) generally showed greater volume increases over one month of abstinence from alcohol than those with less atrophy at baseline, and that smaller lobar WM volumes were associated with greater lobar white matter volume increases with prolonged abstinence. These observations highlight the dynamic neuroplastic changes that can occur after the removal of a chronic insult, such as chronic alcohol abuse.

Although associations between brain volume at baseline and volume changes during alcohol abstinence have been reported, no mathematical formula has been advanced that predicts morphometric changes that occur with sustained abstinence from alcohol. Such a formula could be useful in further understanding abstinence-related brain plasticity, for predicting missing values in longitudinal studies and for predicting the trajectory of brain tissue volume recovery over durations of abstinence that extend beyond the duration of most typical longitudinal neuroimaging studies. Reliable projections of brain volume changes that accompany prolonged (i.e., years of) abstinence could have significant clinical and psycho-educational relevance and fuel future research applications.

In this report, using experimental serial volumetric MRI data from three different time points in the same alcohol-dependent individuals, we propose and demonstrate the utility of a mathematical formula that fairly reliably predicts individual changes in lobar gray matter (GM) or white matter (WM) volumes during abstinence from alcohol. The proposed formula is novel in that the prediction of individual brain volumetric changes is not determined from the generalized behavior of a study group (as in statistical models that incorporate group error terms), but is rather based on repeated measurements in the same individual, therefore

incorporating the unique characteristics of the recovery of the individual's regional brain volumes.

2. Theory

The amount of brain tissue volume (the volumetric sum of neuronal, microglial, glial, interstitial and vascular components) gained at any given time during abstinence in AUD/SUD is dependent on the rate of tissue volume change during abstinence. As the amount of brain tissue gained at a given time is directly proportional to the alcohol or substance induced atrophy at the beginning of abstinence, the rate of tissue volume change at any given time (t) during an interval of abstinence is also directly proportional to the amount of atrophy at t . The amount of atrophy at a given time is inversely related to the volume of brain tissue present at that time (i.e., the greater the atrophy, the lesser the amount of tissue, and vice versa). Accordingly, the rate of change of the tissue volume at t should also be inversely related to the volume of tissue at t . From the foregoing argument it follows that if the volume of brain tissue at t is $V_{(t)}$, and the atrophy is secondary to the effects of the chronically abused substance, then mathematically the rate of tissue volume gain, denoted

by $\left(\frac{dV_{(t)}}{dt}\right)$ at t (measured from the onset of abstinence) can be expressed as:

$$\frac{dV_{(t)}}{dt} \propto \frac{1}{V_{(t)}} \text{ or } \frac{dV_{(t)}}{dt} = \frac{k_i}{V_{(t)}}. \quad (1)$$

Here, k_i is a constant of proportionality unique to the i -th individual that determines the rate of the individual's brain tissue volume change. k_i can be referred to as the i -th individual's 'recovery rate factor'. Factors such as age, genetics, environmental, nutritional, general medical condition etc., which influence brain tissue recovery (or growth), all contribute to the value of the recovery rate factor k_i . It should be noted that this study is not intended to determine how much each of these factors contribute to the value of k_i , but rather to describe the individualized trajectory of the brain tissue recovery process. An implicit assumption is that the same undetermined factors that govern k_i in the fitted interval also govern k_i in the trajectory (i.e., if these factors are significantly different in these two time periods, prediction accuracy will be reduced). Integration of equation (1) yields

$$\frac{1}{2}V_{(t)}^2 = k_i t + C_i, \quad (2)$$

where C_i is a constant of integration for the individual. If t is in days, k is in $\text{volume}^2 \text{ day}^{-1}$ and C in volume^2 . Figure 1 shows a plot of $V_{(t)}$ against t , according to equation (2), using practical values of C and k for frontal GM over an abstinence period of 5 years. The intercept on the $V_{(t)}$ axis equals $(2C_i)^{1/2}$, which, theoretically, is the volume of the tissue at the inception of abstinence

If $V_{(t)}$ is known from volumetric data at two different times t_1 and t_2 , then it follows from equation (2) that

$$k_i = \frac{1}{2(t_2 - t_1)} (V_{(t_2)}^2 - V_{(t_1)}^2) \text{ and } C = \frac{V_{(t_1)}^2}{2} - k_i t_1.$$

Hence, using the estimated values of k_i and C_i , the tissue volume at any other time t can be calculated from equation (2). It is worth noting that equation (2) ignores normal aging effects, which is probably a good approximation for only short-term abstinence (e.g., not more than a year). For longer abstinence periods, it is necessary to add a normal aging factor (λ^2), so that equation (2) becomes:

$$\frac{1}{2}V_{(t)}^2 = k_i t + C_i - \lambda_i^2 \quad (3),$$

where λ_i^2 is the amount of brain tissue the individual lost due to normal aging over the assessment interval. It is best estimated from an age-matched longitudinal control sample. Alternatively, annual rates of regional tissue volume lost due to normal aging have been reported (e.g., (Driscoll et al., 2009; Resnick et al., 2000; Resnick et al., 2003; Scahill et al., 2003)) that λ can be estimated for an individual for a given period of abstinence.

3. Evaluation of the Performance of the Formula

We tested the formula using measured MRI-derived regional brain tissue volumes acquired from 16 abstinent alcohol dependent individuals (13 males, 3 females) with complete regional brain tissue volume measures at three different time points (TP). The participants were between 28 and 66 years of age (50.7 ± 11.9 years, mean \pm standard deviation) and met DSM-IV criteria for alcohol dependence with physiological dependence. The male participants consumed more than 150 alcoholic drinks per month, the female participants more than 80 drinks per month (one standard alcoholic drink contains 13.6 g of pure ethanol) for eight or more years before enrollment into the study. Participants were studied after 5.5 ± 3.0 days (TP1), 36.4 ± 6.8 days (TP2) and 222.3 ± 41.1 days (TP3) of sustained abstinence. All participants gave formal written consent for the research, which was approved by the Institutional Review Boards of the University of California, San Francisco and the San Francisco Veterans Affairs Medical Center. The MRI data were acquired in conjunction with an ongoing neuroimaging project investigating the consequences of alcohol dependence on neurobiological and neurocognitive recovery during abstinence from alcohol. The data were acquired on a 1.5 Tesla clinical MR scanner (Vision, Siemens Medical Systems, Iselin NJ) using T2-weighted oblique-axial imaging (TR/TE₂ = 2500/80 ms, 1×1 mm² in-plane resolution, 3 mm slice thickness, no slice gap) with slices oriented 5° to the orbitomeatal angle as seen on a midsagittal scout and T1-weighted coronal imaging with a Magnetization Prepared Rapid Acquisition Gradient Echo sequence (TR/TI/TE = 9/300/4 ms, 1×1 mm² in-plane resolution, 1.5 mm slabs) oriented orthogonal to the long axis of the hippocampus. Three-tissue intensity based segmentation (based on the well-validated method of Leemput et al. (Van Leemput et al., 1999)), was applied to the T₁-weighted images to assign a set of probabilities of WM, GM, and cerebrospinal fluid (CSF) to each MRI voxel. Intracranial volume (ICV) was calculated for each TP as the sum of all MRI voxels within brain. The mean group difference in ICV for TP1 and TP3 was about 0.2 ml. The T2-weighted images were coregistered and re-sampled to the T1; and used to mask out signal from non-brain tissue.

We evaluated the performance of the formula using volumes for frontal, parietal and temporal GM and WM, denoted here by fGM, pGM, tGM, fWM, pWM and tWM, respectively. Using these lobar volumes for TP1 and TP2 of each participant as inputs, we predicted the corresponding TP3 lobar volumes for each participant. Similarly, using the TP2 and TP3 lobar volumes, we predicted the individual TP1 lobar volumes.

For comparison, we also estimated the individual tissue volumes for TP1 and TP3 using the method of multiple imputations (MI) (PROC MI in SAS, version 9.2) (Schafer, 1999),

which is frequently used for imputing missing data in cost effectiveness analyses (Noble et al., 2010) and in medical research (Sterne et al., 2009). The MI method is thought to be better for imputing missing data than group mean replacement or single imputation methods and can be used on both cross-sectional and longitudinal data (Noble et al., 2010); (Sterne et al., 2009). We did so by first deleting all TP1 values (i.e., setting them to missing) and imputing those now missing ICV-corrected volumes for each participant 10 times using data from TP2 and TP3. Participant age and lifetime mean monthly alcohol consumption were used as covariates as well (as they affect brain tissue volumes); the average of these 10 imputations was then calculated as the individual's imputed tissue volume at TP1. This process was repeated by deleting the TP3 data imputing those values from TP1 and TP2. The predicted data of the regional volumes derived from our formula and from the MI approach were then compared with the experimentally measured volumes for the corresponding TP, using two statistical approaches: i) calculating the percentage difference between measured and predicted/imputed data to compare the performances of the two methods and, ii) calculating intra-class correlations between the measured and predicted/imputed data to compare the degree of similarity between the volume estimates of each method with the corresponding experimentally measured data. We also performed paired t-tests between TP2 observed data and TP3 observed/predicted data and between TP2 observed data and TP1 observed/predicted data to evaluate the degree to which the statistical analysis that used predicted data gives statistical outcomes similar to that using observed data.

4. Results

4.1. Percentage Differences between Measured and Calculated Data

Tables 1 – 3 show the measured volumes and the corresponding volume estimates for TP1 from our formula and the MI for fGM, pGM, and tGM in all 16 participants. For illustrative purposes, Figure 2 shows representative plots of experimental data for each TP and trajectories for lobar GM volumes for eight of the 16 participants. The circular marks, star marks and triangular marks show the measured frontal, parietal and temporal GM volumes for the corresponding TP for each individual. The curves show the trajectories derived from our formula using the TP1 and TP2 volumes as inputs to predict the TP3 volumes for each individual. These plots allow appreciating the small deviation of the estimated individual TP3 volumes from the measured TP3 volumes. For brevity, we did not include GM plots for all 16 participants or corresponding plots and data for lobar WM volumes; instead, we provide results from data of all the participants for both GM and WM analyses in the text.

In Tables 1–3, columns 2, 3, and 4 show the measured volumes (V_{measured}) for TP3, TP2 and TP1 respectively. Columns 5 and 6 show the volume estimates from the formula (V_{formula}) and the multiple imputations (V_{MI}), respectively; and columns 7 and 8 show the percentage difference between V_{measured} and V_{formula} and between V_{measured} and V_{MI} , respectively. The group means ($\text{Mean}_{\text{abs}}\Delta V$) were calculated from the absolute values of individual percentage differences of the predicted volumes from the measured volumes for all 16 participants. For TP1, $\text{Mean}_{\text{abs}}\Delta V1$ for our formula were 0.10, 0.21, 0.39% for fGM, pGM, tGM, respectively, and 0.01, 0.04, and 0.51 % for fWM, pWM and tWM, respectively. The corresponding $\text{Mean}_{\text{abs}}\Delta V3$ for TP3 were 0.42, 1.17, 1.77, 0.17, 0.56, and 2.72 %. For comparison, the corresponding results of the MI approach were as follows: $\text{Mean}_{\text{MI}}\Delta V1$ for TP1 were 2.85, 4.19 3.42, 3.78, 7.49, and 4.07 %; and for TP3, $\text{Mean}_{\text{MI}}\Delta V3$ were 3.78, 4.01, 3.85, 3.77, 7.58 and 4.44 %. For each lobar tissue type, the MI estimates give much larger deviations from the measured volumes than the results obtained by our formula.

Also, as depicted in Figure 2, each curve passes close to the experimental data at TP3, demonstrating that the formula describes the individual time courses of brain volume re-growth very well.

4.2. Intra-class Correlations between Measured and Predicted Data

The intra-class correlation coefficients between V_{measured} and V_{formula} for TP1 were either 0.99 or 0.98 for fGM, pGM, tGM, fWM, pWM and tWM; and the corresponding coefficients for TP3 were 0.98, 0.98, 0.97, 0.98, 0.97 and 0.92, respectively. The coefficients between V_{measured} and V_{MI} were 0.96, 0.88, 0.90, 0.89, 0.68 and 0.85, respectively, for TP1; and 0.91, 0.90, 0.88, 0.92, 0.73 and 0.87, respectively for TP3. Here again, the predictions from our formula show closer relations to the measured data than the MI estimates.

4.3. Paired t-test of Volumes between TPs

Tables 4 and 5, show results of the paired t-tests for TP1 – TP2 and TP2 – TP3 volumes respectively. ‘Pair 1’ and ‘Pair 2’ of each row constitute parallel analyses for the tissue indicated, where ‘Pair 1’ represents paired t-test between ‘TP1 measured’ and ‘TP2 measured’/‘ TP2 measured and TP3 predicted’ data. The predicted data from ‘Pair 2’ yielded t-statistics and P-values very similar to those of the measured data from ‘Pair 1’ for all the tissues except tGM and tWM. The differences in results between the measured and predicted data for tGM and tWM may have to do with temporal lobes experiencing magnetic field distortions and signal loss from susceptibility differences between brain and nearby ear canal, which can lead to inaccurate segmentation.

5. Discussion

The proposed mathematical formula describes the trajectory of regional GM and WM volume recovery in AUD during sustained abstinence from alcohol. The regional brain volumes predicted from the formula very closely approximated the measured volumes for all tissues. Similarly, high consistency between the measured data and the data derived from the formula were reflected in both the high intra-class correlation coefficients and the majority of the paired t-tests. Importantly, the formula accounts for substantial individual variability (through the recovery rate factor k) in the course and magnitude of regional brain tissue volume changes during abstinence from alcohol and does not rely on group data in the way that statistical methods such as MI do. Since it is unclear to what extent age, biological differences, genetic factors and other unknown factors contribute to recovery rates, basing our predictions on correlated volume measures at two time points gives us some protection/immunity against unrealistic estimates. The individually varying recovery rates demonstrated in Figure 2 adversely affect the accuracy of common imputation methods that are based on group data characteristics. The larger deviations of the measured data from that calculated with the common MI approach versus data estimated by our formula support this assertion.

Non-linear Tissue Volume Increases in Abstinent Substance Users

Simple linear trajectories were used previously to estimate brain tissue recovery rates in abstinent alcoholics (Gazdzinski et al., 2005a; Pfefferbaum et al., 1995). However, linear recovery rates contradict research observations that brain volume gains decrease with duration of abstinence and the goodness of fit with our proposed formula. Based on longitudinal MRI volume data over seven months of abstinence from alcohol, we previously suggested that brain tissue volume gains over that time period may be exponential (Gazdzinski et al., 2005a). However, for the recovery process to be exponential, the recovery rate at any time has to be directly proportional to the available brain tissue volume

at that time (i.e., the smaller the available volume, the slower the rate of recovery and vice versa) - this is contrary to observations. Therefore, linear or exponential functions are not expected to describe brain volume recovery processes appropriately, as is indeed observed in our described analyses. On the other hand, our formula better describes brain volume trajectories during short and long term abstinence, because its derivation was based directly on the observations that cross-sectionally, individuals with smaller tissue volumes at the inception of abstinence recover volume faster than those with larger baseline volumes and that longitudinally, short-term recovery rates are greater than long-term recovery rates.

We also tested the formula on lobar volume decreases in individuals with dementia, who had four MRI scans over two years (baseline, six months, 12 months, two years). When using the two initial measurements to calculate the values of C and k in the formula, the deviations of our estimates from the measured data at 12 months and two years were less than 2% and similar for both TPs. It appears important, however, that the initial time interval is long enough to fit volume change reliably (i.e., volume change should be large compared to the measurement error). A case in point is that in our abstinent cohort of alcohol dependent individuals estimates from the formula were much better when predicting TP1 data from TP2 and TP3 data. The input data were separated by a longer scan interval than when predicting TP3 data from TP1 and TP2 data, which were separated by a shorter scan interval. In other words, because MRI volume measures are inherently noisy, coupled with the fact that any physiological changes during abstinence from alcohol are gradual processes, the longer the interval between the two measurements that are used to estimate k , the more accurate k is for predicting volume changes. If the interval between TP measures used to estimate k is not long enough, the performance of our formula is only somewhat better than MI, as demonstrated by the deviations of both methods for the determination of TP3 volumes. The MI results are insensitive to TP intervals (i.e., similar error magnitudes for predicting TP1 and TP3), as the MI approach is based only on the respective TP's group data.

We expect that a similar trajectory of brain tissue volume changes may be apparent in those who remain abstinent from substance(s) other than alcohol. This is because during abstinence from substances, promotion of biological/morphometric homeostasis may be driven by similar basic mechanisms, much more related to factors mediating plasticity than to the nature of the abused substance per se. Such factors and mechanisms of brain regeneration in alcoholism have been described and are thought to mimic general mechanisms involved in brain growth and plasticity (Crews and Nixon, 2009). Brain tissue recovery depends on plastic adaptations, which are likely mediated by a complex interplay among the individuals' genetic/epigenetic factors, chronicity and magnitude of substance use and various environmental circumstances including general health and disposition. Further research in quantitative neuroimaging of abstinent individuals with AUD and SUD is required to confirm this supposition. It is encouraging that the trajectory of longitudinal volume loss in dementia appears also well represented by our formula. Together, these data sets suggest that our formula describes both brain growth and shrinkage well. Furthermore, it is of note that MRI detected brain tissue volume changes with normal human aging/development has been described to follow also a non-linear course (Bartzokis et al., 2001; Ge et al., 2002; Jernigan and Gamst, 2005; Lenroot et al., 2007) as has myelination in several brain regions (Bartzokis et al., 2009; Benes et al., 1994).

Potential Applications

The proposed formula has several potential clinical and research applications. For instance, for effective treatment and monitoring of AUD and SUD patients, it would be highly informative and motivational to have a model that fairly reliably charts the course and level of volume recovery over time. Also, these disorders are characterized by a chronically

relapsing/remitting course over lifetime (Baler and Volkow, 2006) and relapse in AUD is associated with further brain tissue volume loss (Pfefferbaum et al., 1995). However, the degree to which the severity of the relapse is related to the amount of volume lost is unclear (Gazdzinski et al., 2005a). The proposed formula may assist in the prediction of the amount of brain tissue volume lost by an individual due to relapse, by comparing the volume of tissue measured at a given time during relapse to its volume predicted with the formula for that same time, which represents the volume had abstinence been sustained. This will be useful in educating recovering alcohol dependent individuals about the potential neurobiological benefits of abstinence, ultimately increasing their motivation to stay abstinent. The formula could also be useful in determining regional variability in the magnitude of change associated with abstinence or relapse, as suggested by the individually varying recovery rates for GM shown in Figure 2. The application of our formula to longitudinal MRI volumetric data of dementia patients over two years (see above) suggests that brain tissue loss in dementia follows a trajectory reverse to the tissue gain observed during alcohol abstinence. Thus, the proposed formula may also prove useful for estimating missing values in longitudinal studies of dementia and mild cognitive impairment, where brain volume loss with time is widely and promisingly used as a marker of disease progression in clinical trials, but where missing data is fairly common and impeding trial data analyses.

Our Formula versus Multiple Imputations

As demonstrated, this formula fairly accurately calculates missing data points in longitudinal volumetric studies of brain tissue volume recovery in *individuals* abstinent from alcohol (and hypothetically other substances). The conventional statistical imputation methods rely solely on the generalized behavior of a *group* in the estimation of individual missing data for cross-sectional/longitudinal samples, (e.g., (Schafer, 1997)), with the goal to draw accurate inferences from and about population quantities, not to predict accurately individual missing values. Thus, a major drawback of MI or similar modeling approaches is that individual biological differences and other within-subject factors that may affect volumetric changes are obscured, likely contributing to higher estimation errors. Furthermore, conventional modeling methods cannot be used to predict brain volume changes beyond the time frame of the study. Our formula incorporates within the recovery rate factor k , the biological and other characteristics of the individual that influence the recovery process and allow to predict fairly well not only the individual's missing data in a longitudinal data set, but also the brain volume trajectory beyond the duration of the longitudinal study.

Limitations

Limitations of this report are a relatively small sample size and a cohort composed of predominantly male alcohol-dependent individuals. Thus, the study should be considered more of a proof of concept. Second, the demonstration of the goodness of fit with the proposed formula is highly dependent on the quality of the MR data and its tissue segmentation. For instance, poor contrast-to-noise or signal-to-noise and artifacts such as motion can greatly affect image segmentation, which will in turn affect the goodness of the fit of the formula. Also with poor segmentation methods, especially where the segmentation is not consistent across time points, the formula will not give a good fit. Furthermore, it is possible that an individual may experience erratic brain volume recovery due to changes in any of the factors that influence the recovery process and therefore k_i . In such cases the formula will not be accurate as it assumes continuity over the prediction interval. Lastly, we did not test the proposed formula on an independent sample of alcohol dependent individuals. Our promising preliminary results on brain tissue loss in dementia patients however support the assertion that the formula is applicable also to other cohorts.

In conclusion, we have discussed a mathematical formula that fairly accurately predicts the recovery of brain tissue volume in individual long-term abstinent alcoholics. The formula may be applicable to other substances of abuse and to volumetric brain changes in dementia. Therefore, we see important utilities for these volume estimations in clinical trials using repeated neuroimaging volumetrics as outcome measures (whether to observe volume increases or decreases) and in answering research questions about brain tissue growth, plasticity and recovery after discontinuation of a chronic and damaging insult.

Acknowledgments

We thank Drs. Valerie Cardenas, Karl Young, Norbert Schuff, Duygu Tosun, Susanna Fryer and Jong-Min Lee for their various intellectual contributions in the preparation of this manuscript. We also thank the San Francisco VA Medical Center Research Service for logistical support. This work was supported by R01 AA10788 (DJM) and R21 DA025202 (DJM).

References

- Adalsteinsson E, Spielman DM. Spatially resolved two-dimensional spectroscopy. *Magnetic Resonance in Medicine*. 1999; 41:8–12. [PubMed: 10025605]
- Baler RD, Volkow ND. Drug addiction: the neurobiology of disrupted self-control. *Trends Mol Med*. 2006; 12:559–566. [PubMed: 17070107]
- Bartzokis G, Beckson M, Lu PH, Nuechterlein KH, Edwards N, Mintz J. Age-related changes in frontal and temporal lobe volumes in men: a magnetic resonance imaging study. *Arch Gen Psychiatry*. 2001; 58:461–465. [PubMed: 11343525]
- Bartzokis G, Lu PH, Tingus K, Mendez MF, Richard A, Peters DG, Oluwadara B, Barrall KA, Finn JP, Villablanca P, Thompson PM, Mintz J. Lifespan trajectory of myelin integrity and maximum motor speed. *Neurobiology of Aging*. 2009
- Benes FM, Turtle M, Khan Y, Farol P. Myelination of a key relay zone in the hippocampal formation occurs in the human brain during childhood, adolescence, and adulthood. *Arch Gen Psychiatry*. 1994; 51:477–484. [PubMed: 8192550]
- Brody AL, Mandelkern MA, Jarvik ME, Lee GS, Smith EC, Huang JC, Bota RG, Bartzokis G, London ED. Differences between smokers and nonsmokers in regional gray matter volumes and densities. *Biol Psychiatry*. 2004; 55:77–84. [PubMed: 14706428]
- Crews FT, Nixon K. Mechanisms of neurodegeneration and regeneration in alcoholism. *Alcohol Alcohol*. 2009; 44:115–127. [PubMed: 18940959]
- Driscoll I, Davatzikos C, An Y, Wu X, Shen D, Kraut M, Resnick SM. Longitudinal pattern of regional brain volume change differentiates normal aging from MCI. *Neurology*. 2009; 72:1906–1913. [PubMed: 19487648]
- Durazzo TC, Meyerhoff DJ. Neurobiological and neurocognitive effects of chronic cigarette smoking and alcoholism. *Front Biosci*. 2007; 12:4079–4100. [PubMed: 17485360]
- Gazdzinski S, Durazzo TC, Meyerhoff DJ. Temporal dynamics and determinants of whole brain tissue volume changes during recovery from alcohol dependence. *Drug Alcohol Depend*. 2005a; 78:263–273. [PubMed: 15893157]
- Gazdzinski S, Durazzo TC, Studholme C, Song E, Banys P, Meyerhoff DJ. Quantitative brain MRI in alcohol dependence: preliminary evidence for effects of concurrent chronic cigarette smoking on regional brain volumes. *Alcohol Clin Exp Res*. 2005b; 29:1484–1495. [PubMed: 16131857]
- Ge Y, Grossman RI, Babb JS, Rabin ML, Mannon LJ, Kolson DL. Age-related total gray matter and white matter changes in normal adult brain. Part I: volumetric MR imaging analysis. *AJNR Am J Neuroradiol*. 2002; 23:1327–1333. [PubMed: 12223373]
- Jernigan TL, Butters N, DiTraglia G, Schafer K, Smith T, Irwin M, Grant I, Schuckit M, Cermak LS. Reduced cerebral grey matter observed in alcoholics using magnetic resonance imaging. *Alcohol Clin Exp Res*. 1991; 15:418–427. [PubMed: 1877728]
- Jernigan TL, Gamst AC. Changes in volume with age--consistency and interpretation of observed effects. *Neurobiol Aging*. 2005; 26:1271–1274. discussion 1275-8. [PubMed: 16006011]

- Lenroot RK, Gogtay N, Greenstein DK, Wells EM, Wallace GL, Clasen LS, et al. Sexual dimorphism of brain developmental trajectories during childhood and adolescence. *Neuroimage*. 2007; 36:1065–1073. [PubMed: 17513132]
- Liu X, Matochik JA, Cadet JL, London ED. Smaller volume of prefrontal lobe in polysubstance abusers: a magnetic resonance imaging study. *Neuropsychopharmacology*. 1998; 18:243–252. [PubMed: 9509492]
- Noble SM, Hollingworth W, Tilling K. Missing data in trial-based cost-effectiveness analysis: the current state of playdagger. *Health Econ*. 2010
- O'Neill J, Cardenas VA, Meyerhoff DJ. Separate and interactive effects of cocaine and alcohol dependence on brain structures and metabolites: quantitative MRI and proton MR spectroscopic imaging. *Addiction Biology*. 2001; 6:347–361. [PubMed: 11900613]
- Pfefferbaum A, Sullivan EV, Mathalon DH, Shear PK, Rosenbloom MJ, Lim KO. Longitudinal changes in magnetic resonance imaging brain volumes in abstinent and relapsed alcoholics. *Alcohol Clin Exp Res*. 1995; 19:1177–1191. [PubMed: 8561288]
- Pfefferbaum A, Lim KO, Desmond J, Sullivan EV. Thinning of the corpus callosum in older alcoholic men: An MRI study. *Alcoholism: Clinical and Experimental Research*. 1996; 20:752–757.
- Resnick SM, Goldszal AF, Davatzikos C, Golski S, Kraut MA, Metter EJ, Bryan RN, Zonderman AB. One-year age changes in MRI brain volumes in older adults. *Cereb Cortex*. 2000; 10:464–472. [PubMed: 10847596]
- Resnick SM, Pham DL, Kraut MA, Zonderman AB, Davatzikos C. Longitudinal magnetic resonance imaging studies of older adults: a shrinking brain. *J Neurosci Res*. 2003; 23:3295–3301.
- Scahill RI, Frost C, Jenkins R, Whitwell JL, Rossor MN, Fox NC. A longitudinal study of brain volume changes in normal aging using serial registered magnetic resonance imaging. *Arch Neurol*. 2003; 60:989–994. [PubMed: 12873856]
- Schafer, JL. *Analysis of Incomplete Multivariate Data (Monographs on Statistics and Applied Probability 72)*. Vol. Vol.. London: Chapman & Hall/CRC; 1997.
- Schafer JL. Multiple imputation: a primer. *Stat Methods Med Res*. 1999; 8:3–15. [PubMed: 10347857]
- Schroth G, Naegele T, Klose U, Mann K, Petersen D. Reversible brain shrinkage in abstinent alcoholics, measured by MRI. *Neuroradiology*. 1988; 30:385–389. [PubMed: 3211313]
- Sterne JA, White IR, Carlin JB, Spratt M, Royston P, Kenward MG, Wood AM, Carpenter JR. Multiple imputation for missing data in epidemiological and clinical research: potential and pitfalls. *BMJ*. 2009; 338:b2393. [PubMed: 19564179]
- Sullivan E, Rosenbloom MJ, Deshmukh A, Desmond JE, Pfefferbaum A. Alcohol and the cerebellum: Effects on balance, coordination, and cognition. *Alcohol Health & Research World*. 1995; 19:138–141.
- Van Leemput K, Maes F, Vandermeulen D, Suetens P. Automated model-based tissue classification of MR images of the brain. *IEEE Trans Med Imaging*. 1999; 18:897–908. [PubMed: 10628949]
- Zipursky RB, Lim KC, Pfefferbaum A. MRI study of brain changes with short-term abstinence from alcohol. *Alcohol Clin Exp Res*. 1989; 13:664–666. [PubMed: 2688465]

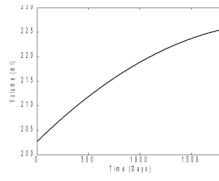


Figure 1.
V(t) against t.

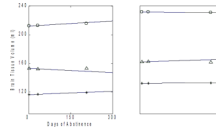


Figure 2.

Plots of frontal, parietal and temporal gray matter volumes against days of abstinence for 8 representative participants. The curves represent our formula's trajectory of volume change with time, using TP1 and TP2 data as input. The circular, star and triangular marks represent the observed data for frontal, parietal and temporal gray matter, respectively.

TP1 volumes: frontal gray matter measured volumes and estimates from formula and multiple imputations for individual study participants

Table 1

Participant	V3 _{measured}	V2 _{measured}	V1 _{measured}	V1 _{formula}	V1 _{MI}	%ΔV _{formula}	%ΔV _{MI}
1	251.96	243.70	242.54	242.60	237.80 ± 8.84	0.03	-1.95
2	230.60	231.53	231.56	231.62	230.27 ± 12.51	0.03	-0.56
3	208.10	203.42	202.03	202.77	204.44 ± 13.13	0.37	1.19
4	215.35	212.87	212.13	212.42	220.91 ± 7.74	0.14	4.14
5	241.39	241.42	239.67	241.43	228.94 ± 8.98	0.74	-4.48
6	269.95	268.15	267.22	267.85	260.29 ± 7.75	0.24	-2.60
7	235.85	238.71	239.57	239.20	249.75 ± 7.62	-0.20	4.21
8	191.69	189.98	189.50	189.60	199.86 ± 10.15	0.05	5.47
9	263.25	258.50	258.01	257.46	250.60 ± 12.02	-0.21	-2.87
10	219.46	218.85	217.86	218.74	219.93 ± 12.29	0.40	0.95
11	206.18	203.51	202.09	202.87	211.30 ± 8.62	0.39	4.56
12	273.65	271.01	271.12	270.59	271.55 ± 7.06	-0.20	0.16
13	212.97	209.21	208.44	208.13	204.41 ± 7.47	-0.15	-1.94
14	236.16	234.22	233.51	233.60	239.69 ± 13.81	0.04	2.65
15	198.14	198.06	197.66	198.04	203.48 ± 7.23	0.19	2.94
16	189.75	189.57	190.10	189.54	199.53 ± 9.14	-0.30	4.96
Mean _{abs} ΔV1						0.23 ± 0.18	2.85 ± 1.65

V3_{measured}, V2_{measured} and V1_{measured} are the experimentally measured data, V1_{formula} = predicted data using the formula, V1_{multi-imp} = estimates from the multiple imputation method;

$$\Delta V1 = \left(\frac{V1_{estimate} - V1_{measured}}{V1_{measured}} \right) \times 100$$

, and Mean_{abs}ΔV1 is the mean of absolute values of the percentage errors.

Table 2

TP1 volumes: parietal gray matter measured volumes and estimates from formula and multiple imputations for individual study participants

Participant	V3 _{measured}	V2 _{measured}	V1 _{measured}	V1 _{formula}	V1 _{MI}	%ΔV _{formula}	%ΔV1 _{MI}
1	141.75	137.82	136.74	137.30	125.35 ± 8.33	0.41	-8.33
2	132.95	132.70	132.69	132.67	122.54 ± 6.06	-0.01	-7.65
3	111.56	110.31	109.95	110.13	114.34 ± 6.21	0.16	3.99
4	119.70	117.25	116.77	116.81	118.63 ± 4.98	0.04	1.59
5	124.09	123.73	123.47	123.63	122.65 ± 5.49	0.13	-0.66
6	138.44	136.47	136.22	136.14	137.48 ± 6.28	-0.06	0.93
7	126.32	128.96	129.06	129.31	133.52 ± 7.60	0.20	3.46
8	106.29	106.53	106.12	106.59	106.83 ± 8.80	0.44	0.67
9	140.48	138.63	137.74	138.23	132.59 ± 8.03	0.36	-3.73
10	116.12	114.86	113.98	114.62	112.88 ± 8.03	0.56	-0.97
11	103.73	102.90	102.83	102.71	114.23 ± 5.94	-0.12	11.09
12	137.34	138.29	137.65	138.43	146.12 ± 4.64	0.57	6.16
13	101.98	101.20	100.72	100.98	109.30 ± 3.84	0.26	8.52
14	130.70	129.71	129.43	129.39	127.11 ± 8.03	-0.03	-1.79
15	109.22	108.42	108.26	108.22	109.16 ± 6.71	-0.03	0.84
16	102.57	102.36	101.76	102.32	108.51 ± 4.25	0.54	6.63
Mean _{obs} ΔV1						0.25 ± 0.20	4.19 ± 3.42

See Table 1 for abbreviations.

Table 3

TP1 volumes: temporal gray matter measured volumes and estimates from formula and multiple imputations for individual study participants

Participant	V3 _{measured}	V2 _{measured}	V1 _{measured}	V1 _{formula}	V1 _{MI}	%ΔV _{formula}	%ΔV _{MI}
1	151.34	149.44	148.01	149.19	148.70 ± 7.72	0.80	0.46
2	162.13	162.65	162.36	162.70	160.63 ± 5.66	0.21	-1.97
3	138.06	135.49	134.25	135.13	140.90 ± 7.25	0.66	5.70
4	153.59	152.62	153.21	152.44	147.03 ± 7.56	-0.50	-4.03
5	167.27	167.71	166.56	167.83	156.24 ± 8.55	0.76	-6.20
6	190.57	186.38	185.80	185.67	185.47 ± 7.76	-0.07	-0.18
7	150.35	150.50	150.55	150.52	157.23 ± 6.39	-0.02	4.44
8	138.39	137.77	136.94	137.63	141.77 ± 7.73	0.51	3.53
9	174.05	173.85	172.69	173.81	166.03 ± 7.33	0.65	-3.86
10	143.72	143.30	143.13	143.22	142.89 ± 5.42	0.07	-0.16
11	145.38	143.20	142.83	142.68	144.37 ± 6.62	-0.11	1.07
12	158.53	158.47	158.76	158.46	168.49 ± 7.71	-0.19	6.13
13	136.63	138.91	137.72	139.55	136.39 ± 4.42	1.33	-0.97
14	174.69	172.26	169.76	171.49	167.87 ± 14.51	1.01	-1.11
15	138.22	138.19	137.67	138.18	132.51 ± 8.51	0.37	-3.75
16	126.14	127.37	126.72	127.60	141.95 ± 5.92	0.69	12.02
Mean _{obs} ΔV1						0.50 ± 0.37	3.42 ± 3.14

See Table 1 for abbreviations.

Table 4

Paired t-tests between TP1 and TP2 data

TP2 volume versus TP1 volume	t statistic	p-value (2-tailed)
<i>fGM</i> : (pair 1): TP2 measured – TP1 measured (pair 2): TP2 measured – TP1 predicted	3.35 3.78	0.004 0.002
<i>fWM</i> : (pair 1): TP2 measured – TP1 measured (pair 2): TP2 measured – TP1 predicted	5.25 3.11	< 0.001 0.007
<i>pGM</i> : (pair 1): TP2 measured – TP1 measured (pair 2): TP2 measured – TP1 predicted	3.84 1.84	0.002 0.086
<i>pWM</i> : (pair 1): TP2 measured – TP1 measured (pair 2): TP2 measured – TP1 predicted	1.05 0.91	0.310 0.380
<i>tGM</i> : (pair 1): TP2 measured – TP1 measured (pair 2): TP2 measured – TP1 predicted	1.53 2.67	0.150 0.032
<i>tWM</i> : (pair 1): TP2 measured – TP1 measured (pair 2): TP2 measured – TP1 predicted	3.40 0.56	0.004 0.580

Table 5

Paired t-tests between TP3 and TP2 data

TP2 volume verse TP3 volume	t statistic	p-value (2-tailed)
<i>fGM</i> : (pair 1): TP3 measured – TP2 measured (pair 2): TP3 predicted – TP2 measured	3.20 2.73	0.006 0.015
<i>fWM</i> : (pair 1): TP3 measured – TP2 measured (pair 2): TP3 predicted – TP2 measured	2.42 4.32	0.029 0.001
<i>pGM</i> : (pair 1): TP3 measured – TP2 measured (pair 2): TP3 predicted – TP2 measured	2.14 3.77	0.049 0.002
<i>pWM</i> : (pair 1): TP3 measured – TP2 measured (pair 2): TP3 predicted – TP2 measured	1.40 1.44	0.183 0.169
<i>tGM</i> : (pair 1): TP3 measured – TP2 measured (pair 2): TP3 predicted – TP2 measured	2.73 2.27	0.016 0.039
<i>tWM</i> : (pair 1): TP3 measured – TP2 measured (pair 2): TP3 predicted – TP2 measured	0.90 3.40	0.382 0.004